

## Comparative Study of Different Immobilization of Strontium in $\text{LiSr}_2(\text{PO}_4)_3$ Crystal through Hydrothermal Process

Y.N. Vaidyanath<sup>1</sup>, K.G. Ashamanjari\*<sup>1</sup>, M. Mylarappa<sup>2</sup>, M.S. Bhargava Ramu<sup>1</sup>, K.R. Vishnu Mahesh\*<sup>3</sup>, S.C. Prashantha<sup>4</sup>, H.P. Nagaswarupa<sup>4</sup>, N. Raghavendra<sup>5</sup>

<sup>1</sup>Department of Studies in Earth Science, University of Mysore, Mysore-570 006

<sup>2</sup>Research Centre, Department of Chemistry, AMC Engineering College, Bengaluru-560083

<sup>3</sup>Department of Chemistry, Dayananda Sagar College of Engineering, Bengaluru-56078

<sup>4</sup>Research Centre, Department of Chemistry, EWIT, Bengaluru-560091

<sup>5</sup>CMRTU, RV College Campus, Bengaluru-560059

\*Corresponding author: leelambike@yahoo.com and vishnumaheshkr@gmail.com

**Abstract:** The main objective of the present study was to synthesis the different immobilization of  $\text{Sr}^{+2}$  in  $\text{LiSr}_2(\text{PO}_4)_3$  crystals using soft hydrothermal method at moderate pressure and temperature conditions. The powder X-ray diffraction confirms that, the synthesized  $\text{LiSr}_2(\text{PO}_4)_3$  material has very good phase purity and crystalline with rhombohedral structure. The energy-disperse X-ray (EDX) spectroscopic analysis shows their elemental composition correlating well with that of the strontium. Observation through a Scanning Electron Microscope (SEM) shows that microstructures of good quality and exhibited smooth surface, sub transparent and sub vitreous lustre. The FTIR studies was used to determine whether the bond structures were affected from the doping or not and revealed that the presence of O-H molecules and minute structural variations of synthesized materials. The TGA graph, temperature vs. weight % loss decreases with increasing the temperature shows Lithium strontium phosphate as thermally stable so it is used as some optoelectronic device applications. The electrical conductivity of  $\text{LiSr}_2(\text{PO}_4)_3$  was investigated as a function of the nature of the transition-metal cation. Impedance measurements show that the materials have relatively good ionic conductance.

**Keywords:** Hydrothermal synthesis,  $\text{LiSr}_2(\text{PO}_4)_3$ , FTIR, Thermal studies, Electrical studies.

### I. Introduction

In modern techno scientific era, the alkali metal phosphates design becomes an important task for developing new compounds for the various industrial applications in electronic devices, as solid electrolytes, sensors, laser materials, piezoelectric, luminescence, opto-electronics, magnetic materials and ceramics [1-2]. To replace the present electrode materials in rechargeable batteries, hundreds of metals, non-metals and compounds have been proposed as probable hosts for energy storage and conversion. Particularly, in a lithium ion battery system, the active materials play a significant role in improving the electrochemical performance of the entire cell.

However, a lot of studies were blindly follow the preparation and improvement of a known compound (such as  $\text{LiMPO}_4$ ) by the same methods, which will hinder the horizon broadening of new materials design [3-4]. Recently, lithium orthometal phosphates, such as  $\text{LiMPO}_4$  (M = Sr, V, Ge, Ti, Sn, Co, Ni, Mn, Zr and Fe) with the olivine-type structures are captivated considerable attention as intercalation electrode materials for rechargeable Li-ion batteries due to their high capacity, high voltage, environmental friendly, cost effectiveness, stable even at over charge and preferable thermal stability during charge-discharge processes [5-12]. The variations in the symmetry of the structures of these compounds are due to the distortion of frameworks caused by introducing various atoms into their framework and different fillings of their cavities have been proposed as potential active materials due to their competitive energy density and excellent thermal stability compared to other spinel-type or layered structured materials [13-15].

The  $\text{LiSr}_2(\text{PO}_4)_3$ ,  $\text{LiFePO}_4$  and  $\text{Li}_3\text{V}_2(\text{PO}_4)_3$  etc., are some of the most prominent representatives, but the electrochemical properties of  $\text{LiSr}_2(\text{PO}_4)_3$  are currently under intensive investigation for several parameters to improve the discharge capacity and capability for energy storage applications. The morphology of a crystal is of great importance because; the properties of a material depend on its size, shape, surface microscopic structure and macroscopic morphology, also influenced by external factors such as level of super saturation, temperature, the solvent, solution purity and addition of a growth modifier to the solution. It is found that, surface morphology of phosphates were highly sensitive and varies widely according to growth techniques, physical-chemical conditions, solution purity, concentration of dopants, concentration of initial components, etc [16-18].

Among many conventional wet chemical routes to synthesize phosphates, hydrothermal method is a very promising alternative technique for producing cathode and anode active materials [18].

In addition, the hydrothermal method is environmentally friendly, fast, simple, and readily scalable by the employment of continuous operation. The unique physical properties of supercritical water, including extremely low viscosity, high reactant diffusivity, zero surface tension, high reactivity, and high supersaturation ratio of reaction intermediates, make it a promising medium to produce highly crystalline and fine sized particles. In the present work, an attempt has been made to synthesize and characterize the different immobilization of Strontium in  $\text{LiSr}_2(\text{PO}_4)_3$  crystals through soft hydrothermal process. Many experiments were carried out using different ratios of LiOH,  $\text{SrCl}_2$ , and 98% of  $\text{H}_3\text{PO}_4$  at moderate temperature. The as prepared samples were used to analyse the thermal properties using TGA and DSC. The electrical behaviour of the samples were investigated by the mixed electronic-ionic conductivity in strontium phosphate containing lithium ions.

## II. Experimental

### 2.1 Preparation of Lithium strontium phosphate ( $\text{LiSr}_2(\text{PO}_4)_3$ ) crystals

A series of  $\text{LiSr}_2(\text{PO}_4)_3$  crystals were synthesized by soft hydrothermal technique at adequate pressure and temperature conditions. The reagents of annular grade (99.99% purity) from Merck Chemicals were used without further purification. Many experiments were carried out using different ratios of LiOH,  $\text{SrCl}_2$ , and 98% of  $\text{H}_3\text{PO}_4$  at constant temperature. The starting reactance were thoroughly mixed at room temperature to get a homogenous, relatively less viscous mixture and were transferred to a Teflon lined stainless steel autoclaves of 50 mL capacity. The synthesis of  $\text{LiSr}_2(\text{PO}_4)_3$  crystals were carried out at temperature range of  $230^\circ\text{C}$ . The nucleation was spontaneous and it was minimized through slow rate of heating. At this temperature, the experiments were run continuously for 5 days and followed by instant quenching to ambient conditions. The resultant product was in semisolid condition. The product was thoroughly washed several times with double distilled water and ethanol using ultrasonic cleaner and final product was filtered and dried under vacuum at  $90^\circ\text{C}$  for 2 hours. The crystals were obtained under following molar ratios in grams.

LiOH (3.75g) +  $\text{SrCl}_2$  (1.875g) +  $\text{H}_3\text{PO}_4$  (9 ml)..... (1)

LiOH (3.75g) +  $\text{SrCl}_2$  (2.35g) +  $\text{H}_3\text{PO}_4$  (9 ml) .....(2)

LiOH (3.75g) +  $\text{SrCl}_2$  (2.6g) +  $\text{H}_3\text{PO}_4$  (9 ml)..... (3)

The synthesis of  $\text{LiSr}_2(\text{PO}_4)_3$  materials to confirmed the reproducibility of the crystals.

### 2.2 Preparation of Pellets

The synthesized sample was crushed into a fine powder and transferred to a stainless-steel die with tungsten carbide lining. After levelling the powder by means of the die position, the whole assembly was placed in a hand-operated hydraulic press. The pellets were prepared by pressing the material at pressure  $8\text{-}10\text{ ton/cm}^2$ . The compactness of the pellet was 80 - 85%. The diameter of the pellets was around 13mm; while the thickness of the pellets usually ranged between 3-5 mm. Thorough cleaning of the die with acetone, before and after use was observed as a usual practice. Pellets were kept in small specimen bottles, which in turn stored in a vacuum desiccator.

### 2.3. Experimental set up for the impedance measurement

It consists of a furnace, a sample holder, and temperature controller and impedance analyser. For the representative compounds of present investigations, the impedance measurements have been carried out as a function of temperature (299 to 449K) and frequency (1 KHz to 1MHz). To measure the electrical conductivity, the flat surface of the cylindrical pellets was polished on different grade of fine polishing papers to remove the surface contaminations and to obtain parallel, smooth surfaces so that the thin silver foils placed over the two-screw blocking thicker silver electrodes adhere well to the specimen. For the loaded sample holder, the tip of the chromel-alumel thermocouple wire has placed in close contact with the sample to measure and control the temperature of the sample. The sample holder was then placed inside the furnace, which was closed at one end to ensure a steady temperature state to be reached.

## III. Result And Discussion

### 3.1 X-ray Diffraction analysis

The phase purity and the crystallinity of the lithium strontium phosphates were observed by powder X-ray diffractometer using the Shimadzu-7000 X-ray diffractometer with monochromatized  $\text{Cu-K}\alpha$  radiation with wavelength  $1.54\text{ \AA}$ . The PXRD spectrum of  $\text{LiSr}_2(\text{PO}_4)_3$  composites were as shown in **Fig 1 (a-c)**. The peaks at  $2\theta$  values of  $15.46^\circ$ ,  $19.51^\circ$ ,  $24.97^\circ$ ,  $27.59^\circ$ ,  $28.61^\circ$ ,  $29.82^\circ$ ,  $34.07^\circ$ ,  $37.10^\circ$ ,  $39.73^\circ$ ,  $42.67^\circ$ ,  $45.50^\circ$ ,  $48.53^\circ$ ,  $50.15^\circ$ ,  $51.77^\circ$ ,  $55.61^\circ$ ,  $58.03^\circ$ ,  $61.27^\circ$ ,  $65.5^\circ$ ,  $72.1^\circ$  corresponded to the crystal planes of (200), (101), (210), (011) (111), (201), (020), (211), (301), (311)(121), (102)(401), (112), (321) (212), (221), (131), (421) (511), (412), (610), (331), (430), (040), (113), (701) and (313) of lithium-strontium phosphate and confirms the well

crystalline rhombohedral phase [19]. The crystallite size (estimated from Scherrer's formula), the dislocation density and stacking fault of as-formed  $\text{LiSr}_2(\text{PO}_4)_3$  were tabulated in Table 1. As the dopant concentration increases, the intensity of (101), (020) and (102) planes decreases and at higher dopant concentration (12V) the sample gets transformed to cubic phase. In addition, from Fig. 1b, it was clearly observed that with the increase of strontium concentration, the diffraction peak slightly shift towards lower angle side may be due to expansion of unit cell volume results in tensile stress, this will certainly change the lattice parameters. All the crystallite size can be evaluated by Scherer's formula as

$$D = \frac{0.9\lambda}{\beta \cos \theta} \dots\dots\dots (1)$$

Where  $\beta$ ; FWHM (in radians),  $\theta$ ; the Bragg angle of the peak,  $\lambda$ ; the X-ray diffraction wavelength, k; 0.90, the constant depends on the grain shape. The dislocation density and stacking fault were estimated by using the relations:

$$\delta = \frac{1}{D^2} \dots\dots\dots (2)$$

$$SF = \left[ \frac{2\pi^2}{45(3\tan\theta)^{1/2}} \right] \dots\dots\dots (3)$$

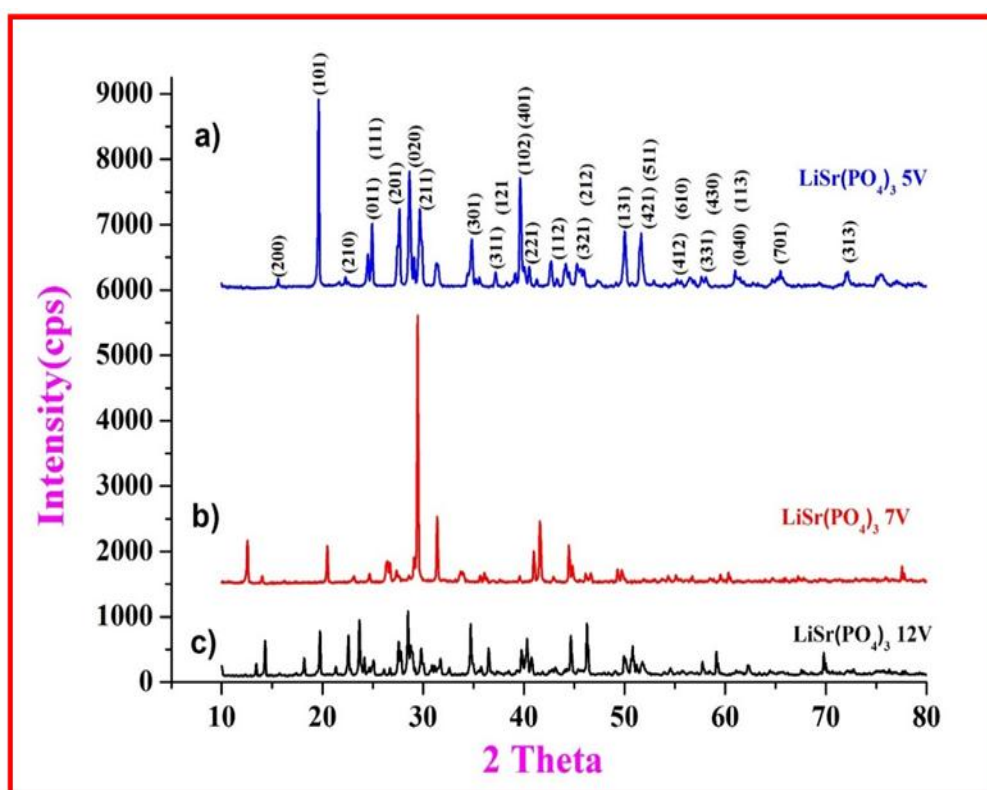


Fig.1. XRD spectra of a)  $\text{LiSr}_2(\text{PO}_4)_3$  5V b)  $\text{LiSr}_2(\text{PO}_4)_3$  7V c)  $\text{LiSr}_2(\text{PO}_4)_3$  12V

**Table 1.** Estimated Crystallite size, strain, stacking fault and dislocation density of different mol ratio of Strontium in  $\text{LiSr}_2(\text{PO}_4)_3$

Sample	FWHM (rad)	Average Crystalline Size (nm)	Strain ( $\epsilon$ ) $\times 10^{-3}$	stacking fault SF	$\delta$ ( $10^5 \text{lin m}^{-2}$ )
$\text{LiSr}_2(\text{PO}_4)_3$ 5 Vol	0.139	59	0.033	0.547	2.80
$\text{LiSr}_2(\text{PO}_4)_3$ 7 Vol	0.137	58	0.034	0.515	2.92
$\text{LiSr}_2(\text{PO}_4)_3$ 12 Vol	0.1906	44	0.046	0.494	5.05

### 3.2 Energy dispersive X-ray spectroscopy (EDAX)

The energy-disperse X-ray (EDX) spectroscopic analysis (in Fig 2a-c) of these samples shows their chemical composition correlating well to that of the strontium. Within the limits of experimental error, the EDAX analytical data on atomic and wt.% of Li, P and Sr are found agreeable with their corresponding expected molar ratios as shown in Table 2. In addition to the peaks corresponding to the elements in the sample,

we also observe weak peaks at 4-6 KeV. However, these are attributed to instrument artifact and are therefore not assigned.

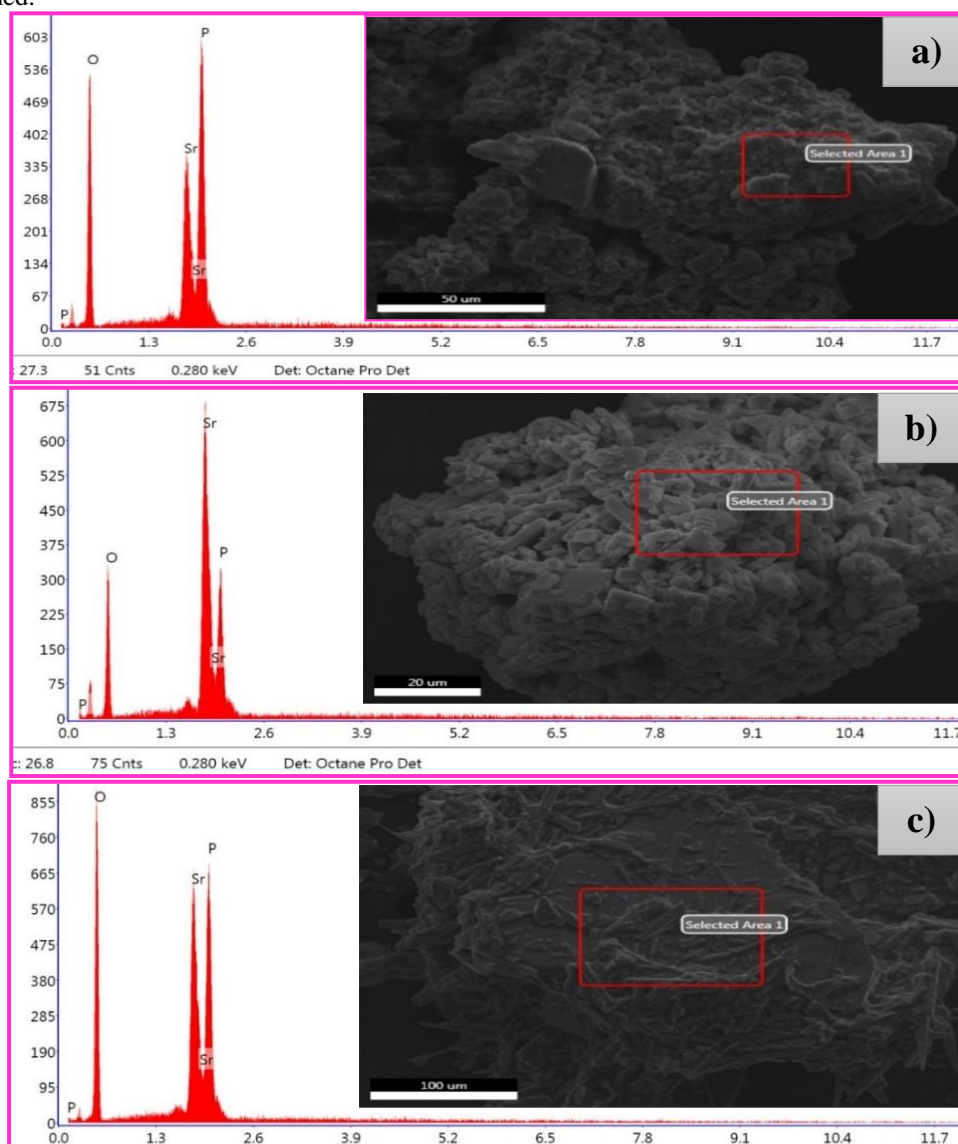


**Fig.2.** EDAX analysis of a)  $\text{LiSr}_2(\text{PO}_4)_3$  5V b)  $\text{LiSr}_2(\text{PO}_4)_3$  7V c)  $\text{LiSr}_2(\text{PO}_4)_3$  12V

**Table 2.** Comparison of the amount of elements added in the reaction mixture of  $\text{LiSr}_2(\text{PO}_4)_3$  with that estimated in the reaction product by EDX.

Sample	Oxygen (%)	Strontium (%)	Phosphor(%)
$\text{LiSr}_2(\text{PO}_4)_3$ 5 V	52.44	19.89	27.67
$\text{LiSr}_2(\text{PO}_4)_3$ 7 V	46.43	27.3	26.27
$\text{LiSr}_2(\text{PO}_4)_3$ 12 V	42.37	38.66	19.0

### 3.3 Scanning Electron Microscope

The morphology and size of the powder was observed using Scanning Electron Microscope (SEM-VEGA3 TESCAN, BMSCE, Bengaluru). Crystals obtained by the hydrothermal method were of good quality and exhibited smooth surface, sub transparent and sub vitreous lustre as shown in **Fig. 3 (a-c)**. It was found that as the Sr concentration increases materials show well-developed morphology with better degree of crystalline nature. Further, increase of Sr concentration in the experiments has not yielded any considerable change either in the morphology or in the size. At the lower concentrations (Figure. 3a), the morphology is by and large

acicular to rhombs, mono-phase. As the concentration of increases, morphology exhibited homogeneous particles with cubic like structure and uniform distribution of fine particles with little agglomeration [20].

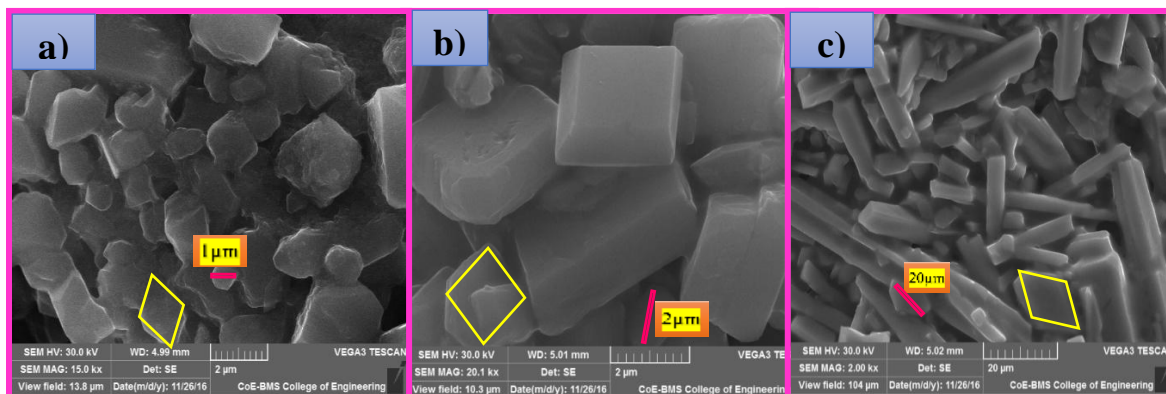


Fig.3. SEM analysis of a)  $\text{LiSr}_2(\text{PO}_4)_3$  5V, b)  $\text{LiSr}_2(\text{PO}_4)_3$  7V, c)  $\text{LiSr}_2(\text{PO}_4)_3$  12V

### 3.4 Fourier Transform -Infrared Radiation Spectroscopy

Fig.4. a-c) show the FTIR spectrum of  $\text{LiSr}_2(\text{PO}_4)_3$  (5V-12 V). FT-IR spectra of samples were recorded in the range  $400$  to  $4000\text{ cm}^{-1}$  at room temperature and is used as a main technique for elucidating the structure of the complexes and enables to understand the radical groups and the minute internal structural distortion also, it was used to determine whether the bond structures were affected from the doping or not. FT-IR spectral studies on alkaline transitional phosphate compounds provide very good information about the formation, structure, distortion of  $[\text{PO}_4]$  tetrahedron, and symmetry of the compounds. The presence of orthophosphate anions in the crystal structure was confirmed with the infrared (IR) spectroscopy. The vibrational modes  $[\text{P}_2\text{O}_7]^{4-}$  were observed in the range  $500$ - $1500\text{ cm}^{-1}$ . The bands in the region of  $1200\text{ cm}^{-1}$  are assigned to the stretching asymmetric vibrations  $\nu_3$ , and bands in the region of  $980$ - $915\text{ cm}^{-1}$  correspond to the stretching symmetric vibrations  $\nu_1$  of the P-O-Pions. Bands in the  $700$ - $400\text{ cm}^{-1}$  assigned to the bending vibrations  $\nu_4$  and  $\nu_2$ . Based on the analysis of the presented IR spectra, we assumed that phosphate of the compositions  $\text{LiSr}_2(\text{PO}_4)_3$  (5V-12 V) to be characterized by the R-3c space group and the prepared samples can be attributed to the orthophosphate class [20 –22].

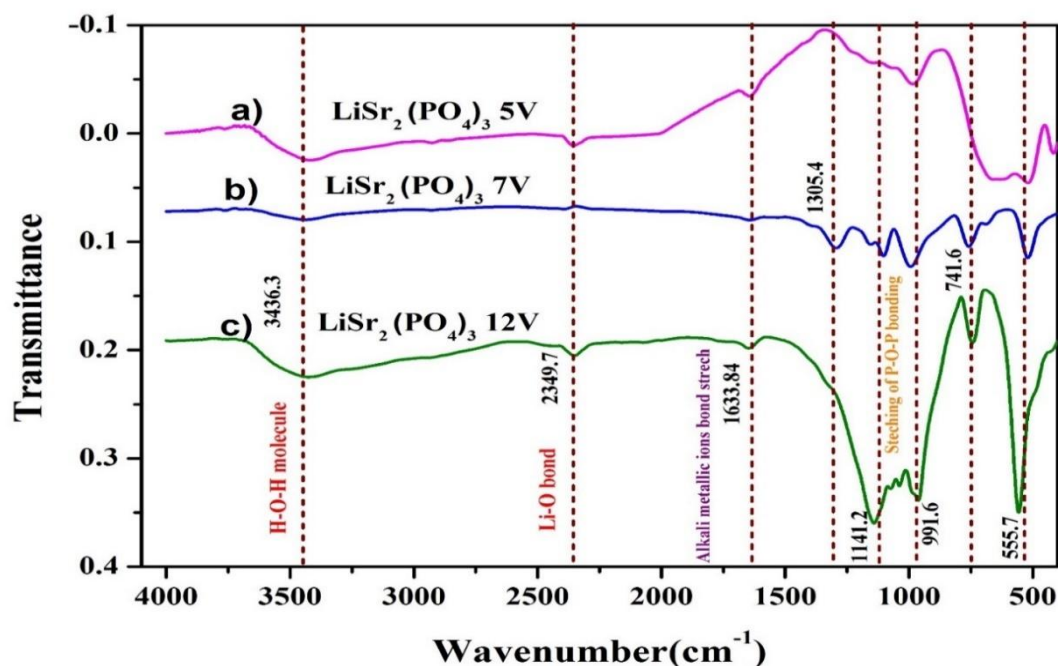


Fig.4. FTIR analysis of a)  $\text{LiSr}_2(\text{PO}_4)_3$  5V b)  $\text{LiSr}_2(\text{PO}_4)_3$  7V c)  $\text{LiSr}_2(\text{PO}_4)_3$  12V

The spectra of  $\text{M}^+\text{Sr}_2(\text{PO}_4)_3$  ( $\text{M}^+ = \text{Li}^+, \text{Na}^+$  and  $\text{K}^+$ ) compounds have exhibited prominent and narrow multiple vibration bands in four frequency regions. The vibration regions at around  $\nu_1=3451\text{cm}^{-1}$ ,  $\nu_2=2350\text{cm}^{-1}$ ,  $\nu_3=1633\text{cm}^{-1}$ , and  $\nu_4=1305\text{cm}^{-1}$ , have clearly indicated the presence of H-O-H molecule. It is clearly noticed that, the study compounds have exhibited more number of splitting and sharpness, especially in the low frequency regions indicating the polymerization of  $[\text{PO}_4]^{3-}$  to  $[\text{P}_2\text{O}_7]^{4-}$ . The above analysis of the vibrations in the related structures of double orthophosphates of Sr and the elements with an oxidation degree of +2 described by different space groups shows that the IR spectra of the phases with large and small cations differ in the character, number, and types of their bands both in the stretching and deformation regions [22].

### 3.5 Thermogravimetric (TG) analysis

Lithium strontium phosphate are very important to soft magnetic materials due to these materials are high magnetic permeability. The TGA thermo grams of  $\text{LiSr}_2(\text{PO}_4)_3$  as shown in Fig.5, the graph temperature v/s. weight % loss decreases with increasing the temperature as observed in the spectra. In this way, the Lithium strontium phosphate was thermally stable so it is used as some optoelectronic device applications. The thermal properties of the  $\text{LiSr}_2(\text{PO}_4)_3$  was studied using differential scanning calorimetry (DSC) from room temperature to  $800^\circ\text{C}$  and the observed thermo grams are shown in the Fig.5. The melting temperature ( $T_m$ ) of  $\text{LiSr}_2(\text{PO}_4)_3$  identified more than  $700^\circ\text{C}$ . Thus, the thermal properties of  $\text{LiSr}_2(\text{PO}_4)_3$  material gives a more information for optoelectronic applications [23].

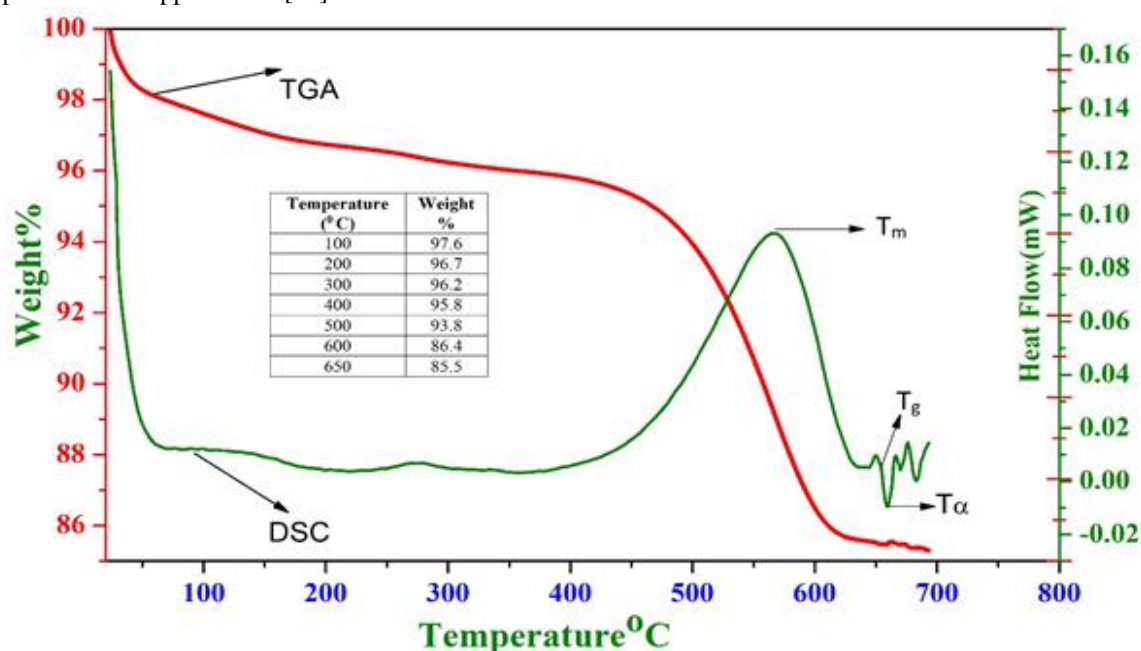


Fig.5. TGA/DSC analysis of  $\text{LiSr}_2(\text{PO}_4)_3$  12V

### 3.6 Electrical Properties

In general, electromagnetic interaction between constituent phases is key point to change dielectric behaviour of material. The dc conductance of sample was measured by Wayne Kerr 6500B impedance analyser with computer interface, where the signal frequency varied from 1 kHz to 10 MHz, equivalent circuit in series and bias voltage set at 1V. Fig.6. show the frequency dependence dc capacitance of  $\text{LiSr}_2(\text{PO}_4)_3$  sample. The frequency response dc capacitance also depends on doping with strontium. Dielectric behaviour has also been studied as a function of temperature (room temperature to  $35^\circ\text{C}$ ). The dielectric measurements were carried out at room temperature in a frequency range using inductance capacitance resistance (LCR) meter bridge (6500B Wayne Kerr). The dielectric constant is calculated from the capacitance value of the given material by the formula

$$\epsilon' = \frac{Cd}{\epsilon_0 A} \dots \dots \dots (2)$$

Where, 'C': capacitance of the pellet in farad,  
 'd' : thickness of pellet in meter,  
 'A' : cross-sectional area of the flat surface of the pellet  
 ' $\epsilon_0$ ' : permittivity constant of free space. ( $\epsilon_0 = 8.85 \times 10^{-12}$  F/m)

Dielectric constant of lithium strontium phosphate was determined by the relation above in Fig. 6 shows representative behaviour of synthesized samples.

At lower frequency, high value of dielectric constant observed and at higher frequency, the dielectric constant decreases. This type of behaviour was observed by several authors [23]. The large value of dielectric constant  $\epsilon'$  for small frequency due to polarization in dielectric structure, porosity, grain boundaries [24]. Better dc conductivity increases the performance of  $\text{LiSr}_2(\text{PO}_4)_3$  in various device application.

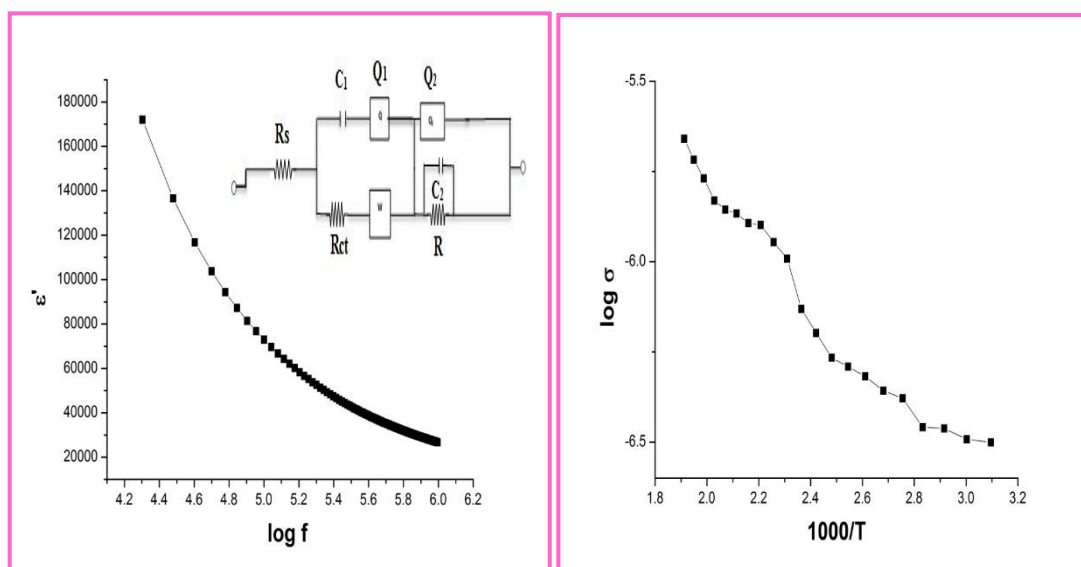


**Fig.6: a)** Variation of  $\epsilon'$  with frequency  $\text{LiSr}_2(\text{PO}_4)_3$  12V  
**b)** Arrhenius plots of the  $\text{LiSr}_2(\text{PO}_4)_3$  12 V -log ( $\sigma_{dc}$ ) vs  $1,000/T$  (K)

#### IV. Conclusion

$\text{LiSr}_2(\text{PO}_4)_3$  crystals were synthesized by soft hydrothermal technique. From XRD, when the concentration of Sr increased, crystallinity also enhanced and the morphology changed from acicular to rhombs. FTIR spectra indicated that there is an increase in the degree of splitting and stretching of the vibration bands, whereas the splitting of vibration bands and polymerization of  $[\text{PO}_4]$  decreased as the Sr (II) ions concentration increased. The TGA/DSC studies revealed that these materials display endothermic reactions due to the liberation of ligands and diffusion. Thermal stability of the materials improved more and more as the strontium concentration increased and the dielectric constant decreases with increasing frequency.

#### References

- [1] I. Hsin Chou and Chin-Feng Fan, Progress in Nuclear Energy 52 (5), 2010, 470-480.
- [2] Ashish Bohre and O.P. Shrivastava, Journal of Nuclear Materials, 433, 2013, 486-493.
- [3] Padhi A.K., Nanjundaswamy K.S., Masquelier C., S and Okada, J.B., Journal of the Electrochemical Society, 144, 1997, 1609.
- [4] P. Tang, N.A and W. Holzwarth, Physical Review B 68, 2003, 165107.
- [5] Jugovic D., and Uskokovic D., Journal of Power Sources, 190, 2009, 538.
- [6] Yi-Ping Liang, Chia-Chen Li, Wen-Jing Chen and Jyh-Tsung Lee, Electrochimica Acta 87, 2013, 763-769
- [7] Padhi A.K., Nanjundaswamy K., and Goodenough J., J. Electrochem. Soc. 144, 1997, 1188-1194.
- [8] Y. Wang, Y. Wang, E. Hosono, K. Wang, H. Zhou, and Angew. Chem. Int. Ed. 47, 2008, 7461-7465.
- [9] Xie H.M., Wang R.S., Ying J.R., Zhang L.Y., Jalbout A.F., Yu H.Y., Yang G.L., Pan X.M., Su Z.M., Adv. Mater. 18, 2006, 2609-2613.
- [10] Wagemaker M., Ellis B.L., Lutzenkirchen-Hecht D., Mulder F.M., Nazar L.F., Chem. Mater. 20, 2008, 6313-6315.
- [11] Li G., Azuma H and Tohda M., Electrochem. Solid-State Lett. 5, 2002, A135-A137.
- [12] Yamada A., Hosoya M., Chung S.C., Kudo Y., Hinokuma K., Liu K.Y and Nishi Y., J. Power Sources 119, 2003, 232-238.
- [13] Yongchao Liu, Shengping Wang, Du Tao, Yu Dai, Jingxian Yu Yongchao Liu, Shengping Wang, Du Tao, Yu Dai and Jingxian Yu Materials Characterization 107, 2015, 189-196
- [14] Huang H., Yin S.C., Kerr T., Taylor N and Nazar L.F., Adv. Mater. 14, 2002, 1525-1528.
- [15] Rui X., Li C., Liu J., Cheng T and Chen C., Electrochim. Acta 55, 2010, 6761-6767.
- [16] Ko Y.N., Koo H.Y., Kim J.H., Yi J.H., Kang Y.C and Lee J.H., J. Power Sources 196, 2011, 6682-6687.
- [17] Qiao Y., Tu J., Xiang J., Wang X., Mai Y., Zhang D. and Liu W., Electrochim. Acta 56, 2011, 4139-4145.
- [18] Rui X., Yesibolati N and Chen C., J. Power Sources 196, 2011, 2279-2282.
- [19] Qiao Y., Tu J., Wang X, Zhang D., Xiang J., Mai Y and C. Gu, J. Power Sources 196, 2011, 7715-7720.
- [20] Ravinder D. and Kumar K. V., Bull. Mat. Sci. 2001, 24, 505.
- [21] Rezlescu N and Rezlescu E., Phys. Stat Sol. (a), 1974, 23, 575.
- [22] Reddy, A. V. R.; Mohan, G. R.; Ravinder, D and Boyanov, B. S, J. Mater. Sci. 1999, 34, 3169.
- [23] El Hiti and M. A. J. Phys. III France, 1996, 6, 1307.
- [24] Dar, M. Abdullah, et al. Journal of Alloys and Compounds 493.1, 2010, 553-560.